

Frustration elimination for effective optical spins in coherent Ising machines

Zheng-Yang Zhou,^{1,2} Clemens Gneiting,^{2,3} J. Q. You,^{4,5,*} and Franco Nori^{2,3,6,†}

¹Department of Physics, Zhejiang Sci-Tech University, Hangzhou 310018, China

²Theoretical Quantum Physics Laboratory, Cluster for Pioneering Research, RIKEN, Wakoshi, Saitama 351-0198, Japan

³Center for Quantum Computing, RIKEN, Wakoshi, Saitama 351-0198, Japan

⁴Zhejiang Province Key Laboratory of Quantum Technology and Device, School of Physics, and State Key Laboratory for Extreme Photonics and Instrumentation, Zhejiang University, Hangzhou 310027, China

⁵College of Optical Science and Engineering, Zhejiang University, Hangzhou 310027, China

⁶Physics Department, The University of Michigan, Ann Arbor, Michigan 48109-1040, USA

(Dated: February 26, 2024)

Frustration, that is, the impossibility to satisfy the energetic preferences between all spin pairs simultaneously, underlies the complexity of many fundamental properties in spin systems, including the computational hardness to determine their ground states. Coherent Ising machines (CIM) have been proposed as a promising analog computational approach to efficiently find different degenerate ground states of large and complex Ising models. However, CIMs also face challenges in solving frustrated Ising models: Frustration not only reduces the probability to find good solutions, but it also prohibits to leverage quantum effects in doing so. To circumvent these detrimental effects of frustration, we show how frustrated Ising models can be mapped to frustration-free CIM configurations by including ancillary modes and modifying the coupling protocol used in current CIM designs. In our proposal, degenerate optical parametric oscillator (DOPO) modes encode the ground state candidates of the studied Ising model, while the ancillary modes enable the autonomous transformation to a frustration-free Ising model that preserves the ground states encoded in the DOPO modes. Such frustration elimination may empower current CIMs to improve precision and to benefit from quantum effects in dealing with frustrated Ising models.

Introduction.—Ising models [1–5] have been widely studied, because these models exhibit, despite of their seemingly simple Hamiltonians, a rich variety of interesting properties, exemplified, e.g., by the theory of spin glasses [6–10]. The price to pay is that the properties of large Ising models with random all-to-all couplings are notoriously difficult to study both experimentally and numerically [11–16]. For instance, finding their ground states is known to be NP-hard.

Coherent Ising machines (CIM) [17–29] have been developed as optical analog computers with the potential to simulate Ising models more efficiently. These machines feature flexible optical couplings, which can in principle be adjusted to realize any desired Ising interaction, overcoming the nearest-neighbor restrictions of other hardware approaches. In particular, this allows them to enter deeply into, and explore, the realm of frustrated Ising problems. Frustrated couplings, which are omnipresent in generic Ising models, lie at the heart of many intriguing properties of Ising models, including the computational hardness of finding ground states [30–36]. Therefore, dealing with frustrated Ising models is a core objective of CIMs.

However, frustrated couplings represent challenges as well for CIMs. Most Ising models with frustrated couplings correspond to CIM configurations where loss acts inhomogeneously on different effective optical spins [37–43], thus breaking the homogeneous-amplitude requirement of CIMs [17]. Moreover, frustration in CIMs results in intrinsic single-photon loss, which decoheres quantum states [44–48] and thus impedes the advancement of

quantum CIMs. Therefore, finding improved ways on how to deal with frustrated couplings can significantly affect the performance of CIMs.

Although frustration is an intrinsic property of generic Ising models, frustrated optical couplings can be circumvented in CIMs while preserving the to-be-found ground states. Since the energy difference between different spin configurations is mapped to the total-loss difference between optical modes in CIMs [17], frustration is absent in CIMs whenever ground states of Ising models are mapped to loss-free optical configurations. Unfortunately, these “zero points”, i.e., the Ising energies corresponding to vanishing optical loss, cannot be adjusted freely in current CIMs.

To solve this obstacle in CIMs, we provide a method to map ground states of frustrated Ising models to lossless optical states with the help of ancillary nondegenerate-optical-parametric-oscillator (NDOPO) modes. In our proposal, the signal degenerate-optical-parametric-oscillator (DOPO) modes express the spin configurations in the same way as in the current CIMs, while the additional ancillas shift the correspondence between Ising energy and optical loss, so that Ising ground states are mapped to lossless optical configurations. Eliminating frustration this way promotes current CIMs mainly in two aspects: First, it allows for the presence of stronger quantum effects in CIMs, e.g., steady states can emerge as superpositions of all the degenerate ground states of the underlying Ising models despite of their frustration. Enabling these quantum effects is essential for developing CIMs operating in the quantum regime. Second, inhomogeneous

geneties caused by frustration are absent, thus improving the performance of CIMs in the semi-classical regime.

Mapping Ising models to CIMs.—In a CIM, the spin states $|\uparrow\rangle$ and $|\downarrow\rangle$ are expressed by coherent states $|\alpha\rangle$ and $|\alpha - \alpha\rangle$, respectively, which are steady states of the uncoupled DOPOs. At the same time, Ising coupling terms,

$$J_{n,m}\sigma_z^{(n)}\sigma_z^{(m)}, \quad (1)$$

are represented by collective loss channels $\mathcal{L}_{m,n}(\rho) = \frac{\Gamma_c}{2}(2L_{n,m}\rho L_{n,m}^\dagger - L_{n,m}^\dagger L_{n,m}\rho - \rho L_{n,m}^\dagger L_{n,m})$, with the Lindblad operator,

$$L_{n,m} = a_n + \text{sign}(J_{m,n})a_m, \quad (2)$$

effectively mapping the energies of different spin configurations to the total loss in the CIM. Here, σ_z^n is the Pauli matrix of the n th spin, $J_{n,m} = \pm J$ with $J > 0$, a_n is the annihilation operator of the n th optical mode in the CIM, and ρ is the density matrix [49].

For $J_{n,m} > 0$, the Ising coupling term (1) contributes a positive energy if the two spins are aligned, and negative energy if they are antialigned. In the corresponding optical coupling (2), the Lindblad term causes loss if the two optical modes have the same phase α , while two optical modes with opposite phases describe a dark state of the loss term. Similarly, if $J_{n,m} < 0$, two optical modes with the same phases describe a dark state of the corresponding loss term.

Therefore, the total energy of a spin configuration, i.e., the summed-up contributions of all the Ising coupling terms (1), is proportional to the total optical loss in the CIM. In particular, the ground state of the Ising model corresponds to the optical configuration with minimum loss. Note that an optical configuration without loss in a CIM corresponds to a spin configuration with minimum possible energy $E_{\text{MPE}} = -JN_c$, where N_c is the total number of coupling terms (1). As the phase transition point (threshold pump power) of a CIM depends on the loss, the optical configuration with minimum loss, which is located at the transition point, can be found by gradually increasing the pump [49]. Remarkably, an Ising model with the ground energy E_{MPE} corresponds to a CIM with vanishing threshold in the absence of unwanted single-photon loss.

Obstacles caused by frustrated couplings.—For illustration, let us consider the simplest possible situation featuring frustration, realized by three DOPO modes, as shown in Fig. 1(a). In this example, all three optical couplings energetically prefer coupled modes with opposite phases, which cannot be simultaneously satisfied by any configuration. Therefore, the system unavoidably sustains loss from at least one coupling channel, thus prohibiting quantum superposition and entanglement. The resulting decoherence represents an intrinsic obstacle for developing quantum CIMs.

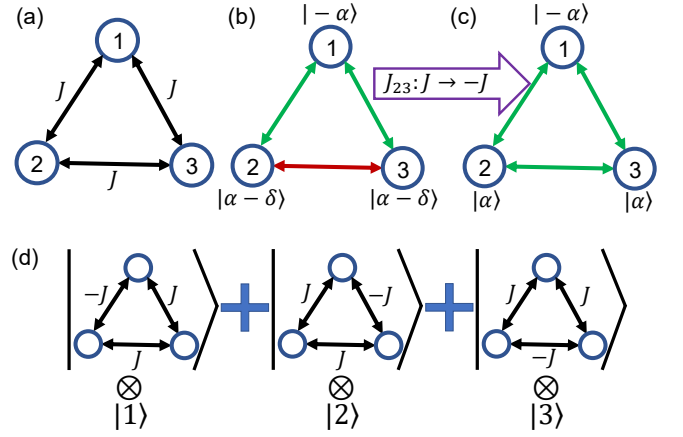


FIG. 1. Illustration of frustration elimination. (a) Paradigmatic three-mode example featuring frustration, reflected by the absence of a dark state. (b) One of the three degenerate ground states of the configuration in (a), sustaining loss due to the coupling between mode 2 and mode 3. The red double-headed arrow represents the coupling contributing loss, and the green double-headed arrows represent the loss-free couplings. (c) Flipping the coupling between modes 2 and 3 eliminates frustration for the ground state in (b). (d) Simultaneous frustration elimination for all degenerate ground states with the help of an ancilla. Although frustration in general prohibits dark states in CIMs, it is possible to map all the ground states of a frustrated Ising model to an optical dark state with the help of ancillary modes.

In addition to suppressing quantum effects, frustration hinders the original function of CIMs, that is, finding ground states of Ising models in the semi-classical regime. In a frustrated CIM configuration, the loss is distributed inhomogeneously among the modes, as illustrated in Fig. 1(b). Consequently, different modes assume different amplitudes, e.g., mode 1 is above threshold while modes 2 and 3 remain below threshold. Such inhomogeneous amplitudes render the mapping in Eqs. (1,2) defective, thus preventing CIMs to find correct solutions [49].

In general, Ising models with ground-state energies larger than E_{MPE} are, in the current CIM design, mapped according to Eqs. (1,2) to such frustrated couplings.

Frustration elimination: the general idea.—For a specific ground state, e.g., $|\alpha - \alpha\rangle|\alpha\rangle|\alpha\rangle$, the loss in the frustrated configuration shown in Fig. 1(b) can be removed by flipping the sign of the lossy coupling term, as shown in Fig. 1(c). However, such direct manipulation cannot take into account all the degenerate ground states of the original Ising model, e.g., it fails for the solution $|\alpha\rangle|\alpha\rangle|\alpha - \alpha\rangle$.

Therefore, we introduce an ancilla that controls the flipping of the coupling terms. As the ancilla, by design, removes the loss, the steady state can then be a superposition of the different solutions, as illustrated in Fig. 1(d) and explicitly verified below. In the resulting state, the ancillary part represents the superposition of

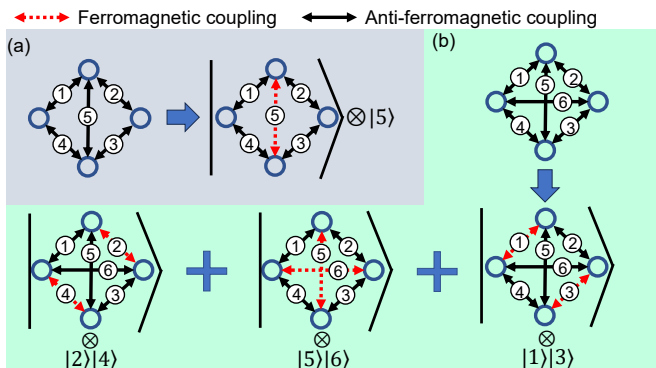


FIG. 2. Frustration elimination in general cases. (a) While the ancilla can flip an arbitrary coupling term, some coupling terms may not contribute to the frustration. The ancilla autonomously identifies a relevant one and flips it. (b) In this fully connected case, flipping a single coupling term is not sufficient to remove the frustration. Two ancillas are required to eliminate the frustration. Following this line of reasoning, frustration elimination can be achieved for any Ising model with appropriate numbers of ancillas.

three different, unfrustrated Ising models, the ground states of which are encoded in the signal modes. The set of these frustration-free ground states comprises all the degenerate ground states of the original frustrated model.

Figure 2 illustrates how to generalize frustration elimination to general frustrated Ising models (1). Flipping an appropriate coupling term, e.g., the coupling 5 in Fig. 2(a), equally reduces the energy by at most $2J$ for all spin configurations, and the ground states of the original model maintain to carry the lowest energy. The lowest energy can be further reduced by flipping several coupling terms, each flip enabled by a separate ancilla as illustrated in Fig. 2(b), while preserving the ground states. Given a sufficient number of ancillary modes, the energy of the ground states E_{ground} can then be reduced to the minimum possible energy E_{MPE} , and the frustration is completely eliminated. Specifically, the number of necessary ancillaries is decided by $(E_{\text{ground}} - E_{\text{MPE}})/(2J)$, which can be identified by either current CIMs or by gradually increasing the number of ancillas.

Ancillary modes in CIMs.—The desired ancillas for frustration elimination can be realized by additional optical modes in CIMs. For a Lindblad operator ($L = a_1 + a_2$) with the dark states $|\alpha\rangle|-\alpha\rangle$ and $|-\alpha\rangle|\alpha\rangle$, the dark states can be modified by including a third mode according to

$$L = a_1 + a_2 + 2a_{\text{an}}. \quad (3)$$

The collective loss in Eq. (3) supports the dark states

$$|\alpha\rangle|\alpha\rangle|-\alpha\rangle_{\text{an}}, \quad \text{and} \quad |-\alpha\rangle|-\alpha\rangle|\alpha\rangle_{\text{an}}, \quad (4)$$

where the two signal modes now take the same sign. Note

that the opposite coupling term ($L = a_1 - a_2$) is equally flipped by this additional ancillary mode.

To control multiple loss channels with one ancillary mode, e.g., the case illustrated in Figs. 1(d) and 2(a), we combine all the loss channels to one channel and connect it to the ancillary mode:

$$L_{\text{an}} = \sum_{n,m} e^{i\phi_{m,n}} [a_n + \text{sign}(J_{m,n})a_m] + 2a_{\text{an}}. \quad (5)$$

Different collective coupling terms are now associated with different phases $\phi_{n,m}$, while the ancillary mode autonomously picks up one phase, e.g., $|\exp(i\phi_{m,n})\alpha\rangle$, and flips the corresponding coupling term. As a simple example, we add a phase term to the loss channel in Eq. (3). The loss channel, $L = (a_1 + a_2)\exp(i\phi) + 2a_{\text{an}}$, has dark states $|\alpha\rangle|\alpha\rangle|-\exp(i\phi)\alpha\rangle_{\text{an}}$ and $|-\alpha\rangle|-\alpha\rangle|\exp(i\phi)\alpha\rangle_{\text{an}}$. To this end, the ancillary modes in Eq. (5) need to be endowed with a phase degree of freedom in addition to the bistable steady states in CIMs.

Such ancillary states can be realized by non-degenerate optical parametric oscillators (NDOPOs) described by the following Hamiltonian and two-photon loss terms:

$$\begin{aligned} H_{\text{NDOPO}} &= S(a_{\text{ani}}a_{\text{ans}} + a_{\text{ani}}^\dagger a_{\text{ans}}^\dagger), \\ L_{\text{NDOPO}} &= a_{\text{ani}}a_{\text{ans}}. \end{aligned} \quad (6)$$

Unlike the case for a DOPO, here two photons generated in the nonlinear process are sent into a signal mode and an idler mode, respectively. The steady states of a NDOPO are also coherent states $|\alpha_{\text{ani}}\rangle|\alpha_{\text{ans}}\rangle$ with $\alpha_{\text{ani}}\alpha_{\text{ans}} = 2S/\Gamma_{\text{NDOPOtp}}$, where Γ_{NDOPOtp} is the two-photon loss rate of the NDOPO. Note that a NDOPO introduces two additional modes a_{ani} and a_{ans} , so that another loss channel as in Eq. (5) with the same loss rate is required,

$$\begin{aligned} L_{\text{ani}} &= \sum_{n,m} e^{i\phi_{m,n}} [a_n + \text{sign}(J_{m,n})a_m] + 2a_{\text{ani}}, \\ L_{\text{ans}} &= \sum_{n,m} e^{-i\phi_{m,n}} [a_n + \text{sign}(J_{m,n})a_m] + 2a_{\text{ans}}, \end{aligned} \quad (7)$$

with $2S/\Gamma_{\text{NDOPOtp}} = |a_n|^2$. To satisfy the two loss channels in Eq. (7) simultaneously, the two NDOPO modes must have amplitudes with the same absolute value, e.g., $a_{\text{ani}} = \exp(i\phi_{m,n})a_n$ and $a_{\text{ans}} = \exp(-i\phi_{m,n})a_n$.

Numerical demonstration of frustration elimination.—We numerically simulate the evolution of the frustration eliminated CIM configuration that corresponds to the frustrated Ising configuration in Fig. 1(a). The three signal modes are described by the DOPO Hamiltonian and corresponding loss terms,

$$\begin{aligned} H_{\text{DOPO}} &= \sum_{k=1}^3 S(a_k a_k + a_k^\dagger a_k^\dagger), \\ L_k &= a_k^2. \end{aligned} \quad (8)$$

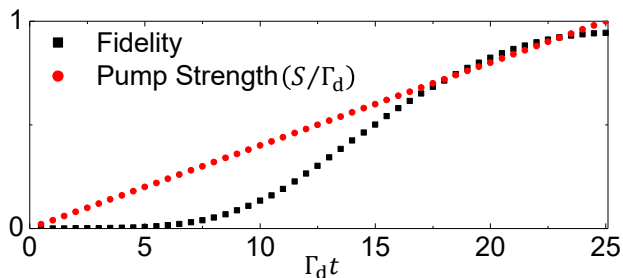


FIG. 3. Ground-state search under frustration elimination for the frustrated Ising configuration presented in Fig. 1. Shown is the time-resolved fidelity of the state, generated with a time-dependent pump, with respect to the pure dark state (9). The latter describes a superposition of the six possible ground states. The numerical demonstration of the close reproduction of (9) convincingly confirms the validity of the mapping of the frustrated Ising model to an optical effective spin system without frustration. The collective loss rate is $\Gamma_c = 3\Gamma$, and the two-photon loss rates for the DOPOs and NDOPOs have the same value ($\Gamma_d = \Gamma_{\text{NDOPOtp}} = \Gamma$).

The DOPOs and NDOPOs share the same two-photon loss rate $\Gamma_d = \Gamma_{\text{NDOPOtp}} = \Gamma$, and the frustration-eliminating loss channels (7) denote three coupling terms with the phases, $\phi_{1,2} = 0$, $\phi_{2,3} = \frac{\pi}{2}$, and $\phi_{3,1} = \frac{\pi}{4}$. The three frustration-eliminated configurations in Fig. 1(d) and the Z_2 symmetry result in a six-component dark state,

$$|\psi(\infty)\rangle = \frac{1}{\sqrt{6} + \delta} \sum_{k=1}^6 |\phi_s^k\rangle \otimes |\psi_{\text{an}}^k\rangle, \quad (9)$$

where the signal mode part $|\phi_s^k\rangle$ encodes the corresponding Ising ground state, while the ancillary part $|\psi_{\text{an}}^k\rangle$ indicates the unsatisfied coupling.

As the dark state in Eq. (9) reduces to the vacuum state for vanishing two-photon pump ($S = 0$), we expect that an initial vacuum state and adiabatically increasing the pump strength S in the spirit of the CIM solution-finding protocol produces the target state (9). The high fidelity (≈ 0.95) with respect to the pure dark state (9) in Fig. 3 implies that the optical effective spin system is not frustrated and resides in a loss-free ground mode. The deviation of the fidelity from 1 can be traced back to nonadiabatic effects and the finite collective loss rate Γ_c . In addition, all the degenerate ground states of the original frustrated model are provided by a superposition state obtained in a single run of the modified CIM setup; exploiting this coherence may improve the efficiency of estimating shared ground state properties, as it has been widely applied in spin systems [50–54].

Realization of the frustration-elimination setup.—The NDOPO modes required in Eq. (6) can be realized with an additional fiber loop, as has been demonstrated in several experiments [55–57]. The modified collective loss terms in Eq. (7) differ from the ones in current

CIMs, which could possibly be realized by delay lines with multiple ports [49]. We stress that the principle underlying frustration elimination does not depend on any quantum effects, allowing it to remain effective in the presence of strong single-photon loss. While the latter in general prohibits the preservation of quantum resources, detrimental amplitude inhomogeneities would still be mitigated if not removed. Therefore, the measurement feedback coupling method based on FPGA chips, which is semi-classical in nature, can support a similar frustration-elimination mechanism.

Generalizing frustration elimination to larger systems requires modifications of the setup described by Eq. (7). For instance, phase fluctuations $\langle e^{i\phi}|\alpha\rangle\langle e^{i\phi'}|\alpha\rangle \neq \delta(\phi - \phi')$ admit only a finite number of phase slots $\phi_{m,n}$ per loss channel within the range $[0, 2\pi)$. In addition, flipping several connections may be necessary in general frustrated models, requiring a matching number of ancillary modes. Under these circumstances, modifications in the frustration-eliminating loss channels may be necessary, but the main idea remains the same for frustration-elimination. [49].

Conclusions.—We have developed a method on how to map frustrated Ising models to optical effective spin systems without frustration, while preserving the set of ground states. In our proposal, the DOPO modes perform, similar to current CIMs, the ground state search, while additional ancillary modes autonomously identify and flip the coupling terms causing frustration. The ancillary modes and switchable couplings can be realized by NDOPO modes and multi-port optical couplings, respectively. As DOPOs and NDOPOs can share the same pump field, our modified CIM can be operated in line with the current protocol, i.e., by gradually increasing the pump intensity. Moreover, our numerical results confirm that the system produces a superposition of all the desired solutions when following the common CIM solution-searching protocol.

Our proposal makes it possible to avoid the intrinsic single-photon loss caused by frustration in the current CIM design, so that the exploitation of loss-vulnerable quantum effects becomes conceivable. Such quantum effects would not only be essential for developing quantum CIMs, but may also help in the solution searching. In addition, other severe problems related to frustration (in particular, detrimental amplitude inhomogeneity) are resolved by frustration elimination. Finally, since our proposal does not rely on quantum effects, its viability is warranted both in the presence of even strong single-photon loss and under the measurement-feedback coupling paradigm.

J.Q.Y. is partially supported by the National Key Research and Development Program of China (Grant No. 2022YFA1405200) and the National Natural Science Foundation of China (NSFC) (Grant No. 92265202 and No. 11934010). C.G. is partially supported by a RIKEN

Incentive Research Grant. F.N. is supported in part by: Nippon Telegraph and Telephone Corporation (NTT) Research, the Japan Science and Technology Agency (JST) [via the Quantum Leap Flagship Program (Q-LEAP)], and the Moonshot R&D Grant Number JP-MJMS2061], the Asian Office of Aerospace Research and Development (AOARD) (via Grant No. FA2386-20-1-4069), and the Office of Naval Research (ONR) (via Grant No. N62909-23-1-2074). Z.Y.Z. is partially supported by the ZSTU intramural grant (23062089-Y) and the National Natural Science Foundation of China (Grants No. 12371135).

* jqyou@zju.edu.cn

† fnori@riken.jp

- [1] Stephen G. Brush, “History of the Lenz-Ising Model,” *Rev. Mod. Phys.* **39**, 883–893 (1967).
- [2] M. W. Johnson and *et. al.*, “Quantum annealing with manufactured spins,” *Nature* **473**, 194 (2011).
- [3] Ronen M. Kroeze, Yudan Guo, Varun D. Vaidya, Jonathan Keeling, and Benjamin L. Lev, “Spinor self-ordering of a quantum gas in a cavity,” *Phys. Rev. Lett.* **121**, 163601 (2018).
- [4] Kirill P. Kalinin and Natalia G. Berloff, “Computational complexity continuum within Ising formulation of np problems,” *Communications Physics* **5**, 20 (2022).
- [5] P. Chandarana, N. N. Hegade, K. Paul, F. Albarrán-Arriagada, E. Solano, A. del Campo, and Xi Chen, “Digitized-counterdiabatic quantum approximate optimization algorithm,” *Phys. Rev. Res.* **4**, 013141 (2022).
- [6] David Sherrington and Scott Kirkpatrick, “Solvable model of a spin-glass,” *Phys. Rev. Lett.* **35**, 1792–1796 (1975).
- [7] M. Mézard, G. Parisi, N. Sourlas, G. Toulouse, and M. Virasoro, “Nature of the spin-glass phase,” *Phys. Rev. Lett.* **52**, 1156–1159 (1984).
- [8] M. B. Weissman, “What is a spin glass? a glimpse via mesoscopic noise,” *Rev. Mod. Phys.* **65**, 829–839 (1993).
- [9] C. L. Baldwin, C. R. Laumann, A. Pal, and A. Scardicchio, “Clustering of nonergodic eigenstates in quantum spin glasses,” *Phys. Rev. Lett.* **118**, 127201 (2017).
- [10] Alba Ramos, Lucas Fernández-Alcázar, Tsampikos Kottos, and Boris Shapiro, “Optical phase transitions in photonic networks: a spin-system formulation,” *Phys. Rev. X* **10**, 031024 (2020).
- [11] Maria Chiara Angelini, Giorgio Parisi, and Federico Ricci-Tersenghi, “Relations between short-range and long-range Ising models,” *Phys. Rev. E* **89**, 062120 (2014).
- [12] Henning Labuhn, Daniel Barredo, Sylvain Ravets, Sylvain de Léséleuc, Tommaso Macrì, Thierry Lahaye, and Antoine Browaeys, “Tunable two-dimensional arrays of single Rydberg atoms for realizing quantum Ising models,” *Nature* **534**, 667 (2016).
- [13] Peter Schauss, “Quantum simulation of transverse Ising models with Rydberg atoms,” *Quantum Science and Technology* **3**, 023001 (2018).
- [14] Andrey Y. Lokhov, Marc Vuffray, Sidhant Misra, and Michael Chertkov, “Optimal structure and parameter learning of Ising models,” *Science Advances* **4**, e1700791 (2018).
- [15] Zeynep Demir Vatansever, “Dynamic phase transitions on the kagome Ising ferromagnet,” *Phys. Rev. E* **106**, 054143 (2022).
- [16] Elijah Pelofske, “Mapping state transition susceptibility in quantum annealing,” *Phys. Rev. Res.* **5**, 013224 (2023).
- [17] Shoko Utsunomiya, Kenta Takata, and Yoshihisa Yamamoto, “Mapping of Ising models onto injection-locked laser systems,” *Opt. Express* **19**, 18091–18108 (2011).
- [18] Zhe Wang, Alireza Marandi, Kai Wen, Robert L. Byer, and Yoshihisa Yamamoto, “Coherent Ising machine based on degenerate optical parametric oscillators,” *Phys. Rev. A* **88**, 063853 (2013).
- [19] Alireza Marandi, Zhe Wang, Kenta Takata, Robert L. Byer, and Yoshihisa Yamamoto, “Network of time-multiplexed optical parametric oscillators as a coherent Ising machine,” *Nature Photonics* **8**, 937–942 (2014).
- [20] Peter L. McMahon, Alireza Marandi, Yoshitaka Haribara, Ryan Hamerly, Carsten Langrock, Shuhei Tamate, Takahiro Inagaki, Hiroki Takesue, Shoko Utsunomiya, Kazuyuki Aihara, Robert L. Byer, M. M. Fejer, Hideo Mabuchi, and Yoshihisa Yamamoto, “A fully programmable 100-spin coherent Ising machine with all-to-all connections,” *Science* **354**, 614–617 (2016).
- [21] Takahiro Inagaki, Yoshitaka Haribara, Koji Igarashi, Tomohiro Sonobe, Shuhei Tamate, Toshimori Honjo, Alireza Marandi, Peter L. McMahon, Takeshi Umeki, Koji Enbutsu, Osamu Tadanaga, Hirokazu Takenouchi, Kazuyuki Aihara, Ken ichi Kawarabayashi, Kyo Inoue, Shoko Utsunomiya, and Hiroki Takesue, “A coherent Ising machine for 2000-node optimization problems,” *Science* **354**, 603–606 (2016).
- [22] Takahiro Inagaki, Kensuke Inaba, Ryan Hamerly, Kyo Inoue, Yoshihisa Yamamoto, and Hiroki Takesue, “Large-scale Ising spin network based on degenerate optical parametric oscillators,” *Nature Photonics* **10**, 415–419 (2016).
- [23] Yoshihisa Yamamoto, Kazuyuki Aihara, Timothee Leleu, Ken-ichi Kawarabayashi, Satoshi Kako, Martin Fejer, Kyo Inoue, and Hiroki Takesue, “Coherent Ising machines-optical neural networks operating at the quantum limit,” *npj Quantum Information* **3**, 49 (2017).
- [24] Atsushi Yamamura, Kazuyuki Aihara, and Yoshihisa Yamamoto, “Quantum model for coherent Ising machines: Discrete-time measurement feedback formulation,” *Phys. Rev. A* **96**, 053834 (2017).
- [25] Naeimeh Mohseni, Peter L. McMahon, and Tim Byrnes, “Ising machines as hardware solvers of combinatorial optimization problems,” *arXiv:2204.00276v1* (2022).
- [26] Christian Leefmans, Avik Dutt, James Williams, Luqi Yuan, Midya Parto, Franco Nori, Shanhui Fan, and Alireza Marandi, “Topological dissipation in a time-multiplexed photonic resonator network,” *Nature Physics* **18**, 442 (2022).
- [27] Sam Reifenstein, Timothee Leleu, Timothy McKenna, Marc Jankowski, Myoung-Gyun Suh, Edwin Ng, Farad Khoyratee, Zoltan Toroczkai, and Yoshihisa Yamamoto, “Coherent SAT solvers: a tutorial,” *Adv. Opt. Photon.* **15**, 385–441 (2023).
- [28] Bo Lu, Chen-Rui Fan, Lu Liu, Kai Wen, and Chuan Wang, “Speed-up coherent Ising machine with a spiking neural network,” *Opt. Express* **31**, 3676–3684 (2023).
- [29] Lin Li, Hongjun Liu, Nan Huang, and Zhaolu Wang,

- “Accuracy-enhanced coherent Ising machine using the quantum adiabatic theorem,” *Opt. Express* **29**, 18530–18539 (2021).
- [30] Steven T. Bramwell and Michel J. P. Gingras, “Spin ice state in frustrated magnetic pyrochlore materials,” *Science* **294**, 1495–1501 (2001).
- [31] T. Kimura, S. Ishihara, H. Shintani, T. Arima, K. T. Takahashi, K. Ishizaka, and Y. Tokura, “Distorted perovskite with e_g^1 configuration as a frustrated spin system,” *Phys. Rev. B* **68**, 060403 (2003).
- [32] R. F. Wang, C. Nisoli, R. S. Freitas, J. Li, W. McConville, B. J. Cooley, M. S. Lund, N. Samarth, C. Leighton, V. H. Crespi, and P. Schiffer, “Artificial ‘spin ice’ in a geometrically frustrated lattice of nanoscale ferromagnetic islands,” *Nature* **439**, 303 (2006).
- [33] Leon Balents, “Spin liquids in frustrated magnets,” *Nature* **464**, 199 (2010).
- [34] K. Kim, M.-S. Chang, S. Korenblit, R. Islam, E. E. Edwards, J. K. Freericks, G.-D. Lin, L.-M. Duan, and C. Monroe, “Quantum simulation of frustrated Ising spins with trapped ions,” *Nature* **465**, 590 (2010).
- [35] J. Struck, C. Ölschläger, R. Le Targat, P. Soltan-Panahi, A. Eckardt, M. Lewenstein, P. Windpassinger, and K. Sengstock, “Quantum simulation of frustrated classical magnetism in triangular optical lattices,” *Science* **333**, 996–999 (2011).
- [36] Cristiano Nisoli, Roderich Moessner, and Peter Schiffer, “Colloquium: Artificial spin ice: Designing and imaging magnetic frustration,” *Rev. Mod. Phys.* **85**, 1473–1490 (2013).
- [37] Hiromasa Sakaguchi, Koji Ogata, Tetsu Isomura, Shoko Utsunomiya, Yoshihisa Yamamoto, and Kazuyuki Aihara, “Boltzmann sampling by degenerate optical parametric oscillator network for structure-based virtual screening,” *Entropy* **18**, 365 (2016).
- [38] Timothée Leleu, Yoshihisa Yamamoto, Peter L. McMahon, and Kazuyuki Aihara, “Destabilization of local minima in analog spin systems by correction of amplitude heterogeneity,” *Phys. Rev. Lett.* **122**, 040607 (2019).
- [39] Ryan Hamerly, Takahiro Inagaki, Peter L. McMahon, Davide Venturelli, Alireza Marandi, Tatsuhiko Onodera, Edwin Ng, Carsten Langrock, Kensuke Inaba, Toshimori Honjo, Koji Enbutsu, Takeshi Umeki, Ryoichi Kasahara, Shoko Utsunomiya, Satoshi Kako, Ken ichi Kawarabayashi, Robert L. Byer, Martin M. Fejer, Hideo Mabuchi, Dirk Englund, Eleanor Rieffel, Hiroki Takesue, and Yoshihisa Yamamoto, “Experimental investigation of performance differences between coherent Ising machines and a quantum annealer,” *Science Advances* **5**, eaau0823 (2019).
- [40] Satoshi Kako, Timothée Leleu, Yoshitaka Inui, Farad Khoyratee, Sam Reifenstein, and Yoshihisa Yamamoto, “Coherent Ising machines with error correction feedback,” *Advanced Quantum Technologies* **3**, 2000045 (2020).
- [41] Fabian Böhm, Diego Alonso-Urquijo, Guy Verschaffelt, and Guy Van der Sande, “Noise-injected analog Ising machines enable ultrafast statistical sampling and machine learning,” *Nature Communications* **13**, 5847 (2022).
- [42] Yoshitaka Inui, Mastiyage Don Sudeera Hasaranga Gunathilaka, Satoshi Kako, Toru Aonishi, and Yoshihisa Yamamoto, “Control of amplitude homogeneity in coherent Ising machines with artificial zeeman terms,” *Communications Physics* **5**, 154 (2022).
- [43] Edwin Ng, Tatsuhiko Onodera, Satoshi Kako, Peter L. McMahon, Hideo Mabuchi, and Yoshihisa Yamamoto, “Efficient sampling of ground and low-energy Ising spin configurations with a coherent Ising machine,” *Phys. Rev. Res.* **4**, 013009 (2022).
- [44] Wei Qin, Adam Miranowicz, Peng-Bo Li, Xin-You Lü, J. Q. You, and Franco Nori, “Exponentially enhanced light-matter interaction, cooperativities, and steady-state entanglement using parametric amplification,” *Phys. Rev. Lett.* **120**, 093601 (2018).
- [45] M. Mamaev, L. C. G. Govia, and A. A. Clerk, “Dissipative stabilization of entangled cat states using a driven Bose-Hubbard dimer,” *Quantum* **2**, 58 (2018).
- [46] R. Y. Teh, P. D. Drummond, and M. D. Reid, “Overcoming decoherence of Schrödinger cat states formed in a cavity using squeezed-state inputs,” *Phys. Rev. Research* **2**, 043387 (2020).
- [47] Ye-Hong Chen, Wei Qin, Xin Wang, Adam Miranowicz, and Franco Nori, “Shortcuts to adiabaticity for the quantum Rabi model: Efficient generation of giant entangled cat states via parametric amplification,” *Phys. Rev. Lett.* **126**, 023602 (2021).
- [48] Zheng-Yang Zhou, Clemens Gneiting, J. Q. You, and Franco Nori, “Generating and detecting entangled cat states in dissipatively coupled degenerate optical parametric oscillators,” *Phys. Rev. A* **104**, 013715 (2021).
- [49] See Supplemental Material at [URL will be inserted by publisher] for detailed discussions and examples.
- [50] Jian Ma, Xiaoguang Wang, C P Sun, and Franco Nori, “Quantum spin squeezing,” *Physics Reports* **509**, 89 C165 (2011).
- [51] Onur Hosten, Nils J Engelsen, Rajiv Krishnakumar, and Mark A Kasevich, “Measurement noise 100 times lower than the quantum-projection limit using entangled atoms,” *Nature* **529**, 505 C508 (2016).
- [52] Luca Pezzè, Augusto Smerzi, Markus K. Oberthaler, Roman Schmied, and Philipp Treutlein, “Quantum metrology with nonclassical states of atomic ensembles,” *Rev. Mod. Phys.* **90**, 035005 (2018).
- [53] Kunkun Wang, Xiaoping Wang, Xiang Zhan, Zhihao Bian, Jian Li, Barry C. Sanders, and Peng Xue, “Entanglement-enhanced quantum metrology in a noisy environment,” *Phys. Rev. A* **97**, 042112 (2018).
- [54] Han Bao, Shenchao Jin, Junlei Duan, Suotang Jia, Klaus Mølmer, Heng Shen, and Yanhong Xiao, “Retrodiction beyond the Heisenberg uncertainty relation,” *Nature Communications* **11**, 5658 (2020).
- [55] Alexander W. Bruch, Xianwen Liu, Joshua B. Surya, Chang-Ling Zou, and Hong X. Tang, “On-chip $\chi^{(2)}$ microring optical parametric oscillator,” *Optica* **6**, 1361–1366 (2019).
- [56] Arkadev Roy, Saman Jahani, Qiushi Guo, Avik Dutt, Shanhui Fan, Mohammad-Ali Miri, and Alireza Marandi, “Nondissipative non-Hermitian dynamics and exceptional points in coupled optical parametric oscillators,” *Optica* **8**, 415–421 (2021).
- [57] Arkadev Roy, Saman Jahani, Carsten Langrock, Martin Fejer, and Alireza Marandi, “Spectral phase transitions in optical parametric oscillators,” *Nature Communications* **12**, 835 (2021).

Supplemental Material for: Frustration elimination for effective optical spins in coherent Ising machines

Zheng-Yang Zhou,^{1,2} Clemens Gneiting,^{2,3} J. Q. You,^{4,5,*} and Franco Nori^{2,3,6,†}

¹*Department of Physics, Zhejiang Sci-Tech University, Hangzhou 310018, China*

²*Theoretical Quantum Physics Laboratory, Cluster for Pioneering Research, RIKEN, Wakoshi, Saitama 351-0198, Japan*

³*Center for Quantum Computing, RIKEN, Wakoshi, Saitama 351-0198, Japan*

⁴*Zhejiang Province Key Laboratory of Quantum Technology and Device, School of Physics, and State Key Laboratory for Extreme Photonics and Instrumentation, Zhejiang University, Hangzhou 310027, China*

⁵*College of Optical Science and Engineering, Zhejiang University, Hangzhou 310027, China*

⁶*Physics Department, The University of Michigan, Ann Arbor, Michigan 48109-1040, USA*

*jyou@zju.edu.cn

†fnori@riken.jp

I. MAPPING ISING MODELS TO COHERENT ISING MACHINES

The basic structure of a CIM is a fiber cavity complemented by a nonlinear crystal and a coupling module. Optical pulses propagate in the cavity and form degenerated optical parametric oscillators (DOPOs) described by a two-photon pump (in the interaction picture),

$$H = -iS \sum_n [(a_n^\dagger)^2 - (a_n)^2], \quad (\text{S1})$$

and loss terms including two-photon loss,

$$\mathcal{L}_{\text{tp}}(\rho) = \sum_n \frac{\Gamma_{\text{tp}}}{2} [2a_n a_n \rho(t) a_n^\dagger a_n^\dagger - \{a_n^\dagger a_n^\dagger a_n a_n, \rho(t)\}], \quad (\text{S2})$$

and single-photon loss,

$$\mathcal{L}_s(\rho) = \sum_n \frac{\Gamma_s}{2} [2a_n \rho(t) a_n^\dagger - \{a_n^\dagger a_n, \rho(t)\}], \quad (\text{S3})$$

where a_n is the annihilation operator of the n th DOPO mode, $\{\bullet, \bullet\}$ denotes the anti-commutator, and ρ is the density matrix describing all the DOPO modes. The DOPO exhibits a phase transition at

$$2|S| = \Gamma_s, \quad (\text{S4})$$

where the steady-state transitions from a squeezed vacuum state to two possible coherent states [1, 2]:

$$|\Psi(t \rightarrow \infty)\rangle = |\pm \alpha\rangle. \quad (\text{S5})$$

CIMs use these two coherent states to emulate spin states:

$$|\alpha\rangle \longleftrightarrow |\uparrow\rangle, \quad |-\alpha\rangle \longleftrightarrow |\downarrow\rangle. \quad (\text{S6})$$

If there are N DOPO pulses in the CIM, the steady state is a collective mode corresponding to a many-body spin system, e.g.,

$$|\alpha\rangle \otimes |-\alpha\rangle \cdots \otimes |\alpha\rangle \longleftrightarrow |\uparrow\rangle \otimes |\downarrow\rangle \cdots \otimes |\uparrow\rangle.$$

Note that a DOPO exhibits dark states if the single-photon loss rate is vanishing ($\Gamma_s \approx 0$):

$$|\Psi(t \rightarrow \infty)\rangle = C_+|\alpha\rangle + C_-|-\alpha\rangle, \quad (\text{S7})$$

and the complex amplitude α of the coherent states is given by $\alpha = i\sqrt{2S/\Gamma_d}$.

Two common design principles for implementing the optical coupling in CIMs are the optical delay-line architecture [3] and the measurement-feedback architecture [4], respectively. The optical delay-line coupling between two DOPO modes can be described by a collective loss,

$$\begin{aligned} \mathcal{L}_{m,n}(\rho) &= \frac{\Gamma_c}{2}(2L_{n,m}\rho L_{n,m}^\dagger - L_{n,m}^\dagger L_{n,m}\rho - \rho L_{n,m}^\dagger L_{n,m}), \\ L_{n,m} &= a_n + \text{sign}(J_{m,n})a_m. \end{aligned} \quad (\text{S8})$$

where n and m correspond to two different DOPO modes. This phase-dependent loss in Eq. (S8) can be associated with an Ising interaction term:

$$H_{n,m} = J_{m,n}\sigma_z^{(n)}\sigma_z^{(m)}, \quad (\text{S9})$$

where $\sigma_z^{(n)}$ is the Pauli matrix of the n th spin, and the coupling strength satisfies $|J_{m,n}| = J$. The effect of the collective loss and of the Ising interaction, respectively, are summarized in the following table:

	Effect	States	Values
Collective loss	Photon loss probability	$ \alpha\rangle_n \otimes \alpha\rangle_m$	$2 \alpha_n ^2\Gamma_c(1 + \text{sign}(J_{m,n}))$
		$ \alpha\rangle_n \otimes -\alpha\rangle_m$	$2 \alpha_n ^2\Gamma_c(1 - \text{sign}(J_{m,n}))$
		$ -\alpha\rangle_n \otimes -\alpha\rangle_m$	$2 \alpha_n ^2\Gamma_c(1 + \text{sign}(J_{m,n}))$
		$ -\alpha\rangle_n \otimes \alpha\rangle_m$	$2 \alpha_n ^2\Gamma_c(1 - \text{sign}(J_{m,n}))$
Ising interaction	Energy shift	$ \uparrow\rangle_n \otimes \uparrow\rangle_m$	$J_{m,n}$
		$ \uparrow\rangle_n \otimes \downarrow\rangle_m$	$-J_{m,n}$
		$ \downarrow\rangle_n \otimes \downarrow\rangle_m$	$J_{m,n}$
		$ \downarrow\rangle_n \otimes \uparrow\rangle_m$	$-J_{m,n}$

It is straightforward to see that the energy difference in the spin system is mapped to the loss difference in DOPO modes. An Ising energy $-J$ corresponds to vanishing loss, while an Ising energy J corresponds to finite loss. Due to the loss-dependent phase

transition in Eq. (S4), the Ising ground state is mapped to a collective DOPO mode with lowest transition pump strength $|S|$.

The measurement-feedback coupling can be expressed as classical pumps on different DOPO modes:

$$H_{\text{MF}} = -i \sum_{n,m} \Omega \text{sign}(J_{n,m}) \langle (a_m + a_m^\dagger) \rangle (a_n - a_n^\dagger). \quad (\text{S10})$$

Such a pump can effectively modify the two-photon pump strength S in the semiclassical limit (mean field):

$$\begin{aligned} H + H_{\text{MF}} &= -iS \sum_n [(a_n^\dagger)^2 - (a_n)^2] - i \sum_{n,m} \Omega \text{sign}(J_{n,m}) \langle (a_m + a_m^\dagger) \rangle (a_n - a_n^\dagger) \\ &\approx -i \sum_n [S \langle (a_n + a_n^\dagger) \rangle - \sum_m \Omega \text{sign}(J_{n,m}) \langle (a_m + a_m^\dagger) \rangle] (a_n^\dagger - a_n). \end{aligned} \quad (\text{S11})$$

As the steady states of DOPOs are coherent states with 0 phase or π phase, we have

$$\langle (a_n + a_n^\dagger) \rangle = \pm \langle (a_m + a_m^\dagger) \rangle,$$

in the semi-classical limit. Here, we assume a negative S to make the amplitude α real. If

$$\langle (a_n + a_n^\dagger) \rangle = \text{sign}(J_{n,m}) \langle (a_m + a_m^\dagger) \rangle,$$

the total pump strength acting on the n th mode is increased. For an opposite relative phase

$$\langle (a_n + a_n^\dagger) \rangle = -\text{sign}(J_{n,m}) \langle (a_m + a_m^\dagger) \rangle,$$

the total pump strength acting on the n th mode is reduced. According to the threshold relation in Eq. (S4), modifying the pump strength of the collective mode is equivalent to modifying the loss of the collective mode. Therefore, the measurement-feedback in Eq. (S11) can also be mapped to the Ising interaction.

II. PROBLEMS CAUSED BY FRUSTRATION

A. Intrinsic loss

In the collective loss coupling protocol, the Ising energy is mapped to the loss. Note that a collective loss with zero loss (that is, the system is in a dark state) corresponds to a spin

configuration in which all the Ising coupling terms contribute negative energies. Such spin configurations do not exist in frustrated Ising models. Therefore, there will be intrinsic loss caused by the coupling protocol, if we use CIMs to simulate frustrated Ising models. Such intrinsic loss generically destroys most strong quantum effects, and thus prevents CIMs benefiting from quantum effects. Note that the current measurement-feedback coupling protocol exhibits few quantum effects.

B. Inhomogeneity in amplitudes

Although the current CIMs mainly work in the semi-classical regime, frustration can still cause problems. To correctly map an Ising model to a CIM, the amplitudes of different steady-state DOPO pulses are required to be the same. To see how inhomogeneous amplitudes can cause errors, let us, for example, consider a pair of spins,

$$|\uparrow\rangle_n \otimes |\uparrow\rangle_m,$$

which has the Ising coupling energy $-J$ for the coupling term

$$H_{n,m} = -J\sigma_z^n \sigma_z^m.$$

However, the collective DOPO mode

$$|\alpha\rangle_n \otimes |\alpha + \Delta\rangle_m,$$

is not a dark mode of the collective loss operator,

$$L_{n,m} = a_n - a_m.$$

In addition the effective pump strength shift in Eq. (S11) requires that

$$|\langle\langle a_m + a_m^\dagger \rangle\rangle| = |\langle\langle a_n + a_n^\dagger \rangle\rangle|.$$

Note that one possible approach to mitigate the problem of inhomogeneous amplitudes is the chaotic amplitude control [5].

III. REALIZATION OF FRUSTRATION-ELIMINATION-TYPE COLLECTIVE LOSS

A. Two-mode collective loss with optical delay lines

We first consider a two-mode collective loss formed by a delay line coupled to two optical pulses, as illustrated in Fig. 1,

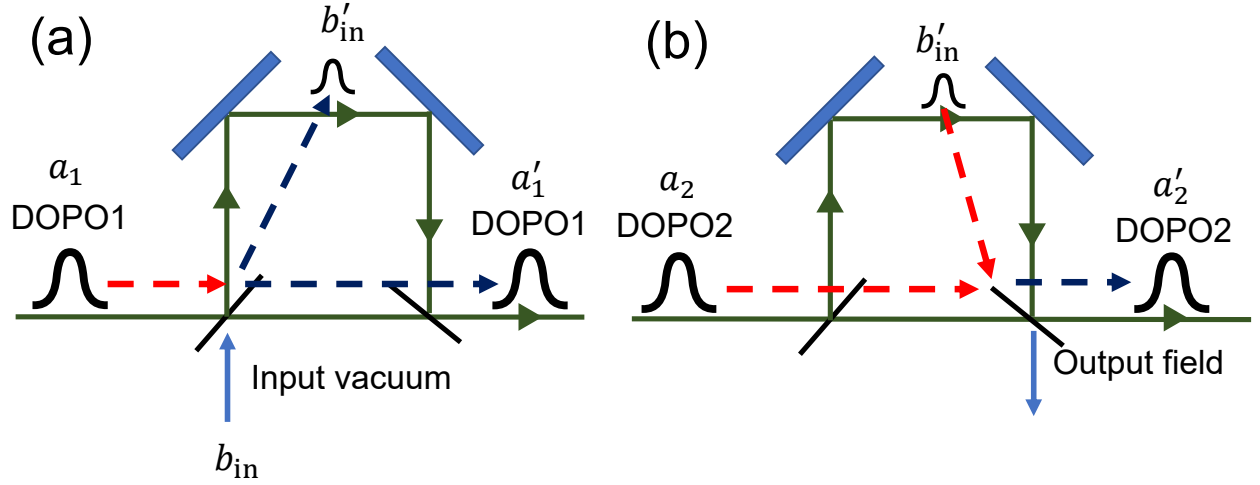


FIG. 1: Illustration of the collective loss realized through delay-line coupling. First, the first pulse denoted as a_1 passes the first beam splitter and mixes with a vacuum field denoted as b_{in} in the delay line denoted as b'_{in} . Then the pulse b'_{in} , which carries the information of a_1 , interacts with the second pulse a_2 at the second beam splitter. For a proper collective state, the output field is almost a vacuum state, which corresponds to a dark state of such collective loss.

The input mode b_{in} (usually the vacuum state) couples with two system modes successively through two beam splitters. The fields after the scattering in Fig. 1(a) are:

$$\begin{aligned} b'_{in} &= T b_{in} + R a_1, \\ a'_1 &= T a_1 - R b_{in}. \end{aligned} \quad (S12)$$

After the second scattering, the fields are:

$$\begin{aligned} b''_{in} &= T^2 b_{in} + R T a_1 + R a_2, \\ a'_1 &= T a_1 - R b_{in}, \\ a'_2 &= T a_2 - R T b_{in} - R^2 a_1. \end{aligned} \quad (S13)$$

Here, the transmission rate is T^2 and the reflection rate is R^2 . When the transmission rate is close to 1, the input mode b_{in} is not coupled to the collective mode $(a_1 - a_2)$ up to the second order of $|R|$. The change of the “dark mode” is as follows:

$$\begin{aligned} a'_1 - a'_2 &= T(a_1 - a_2) + (1 - T)Rb_{\text{in}} + R^2a_1 \\ &= (T + 0.5R^2)(a_1 - a_2) + (1 - T)Rb_{\text{in}} + 0.5R^2(a_1 + a_2). \end{aligned} \quad (\text{S14})$$

It is easy to see that this “dark mode” is not really dark, but coupled to the bright mode $(a_1 + a_2)$ up to second order in R . Therefore, we can conclude that the “dark mode” in Fig. 1(a) is dark to the input field b_{in} , but not completely decoupled from other modes. Note that the second order of R is important because the loss generated by the delay line on the bright mode is of the order of R^2 .

To solve this problem, we can introduce a delay line with opposite scattering order, as shown in Fig. 2. Such a delay line has the following effects on the DOPO pulses:

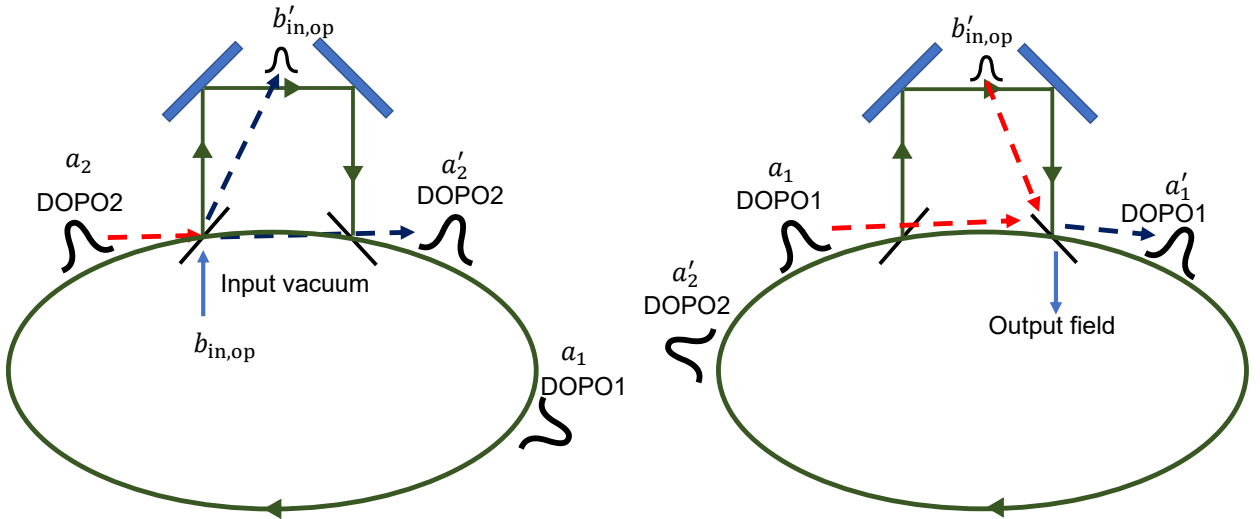


FIG. 2: Illustration of the open-port delay line in the opposite direction. A delay line can only delay and convey the information of a pulse to the pulses coming after it. However, note that in cyclic structures, e.g., in CIMs, the n th pulse in the m th circle passes the coupling modula before the $(n - 1)$ th pulse in the $(m + 1)$ th circle. Therefore, a delay line in the opposite direction delays the pulses longer than the circling period.

$$\begin{aligned} a''_2 &= Ta'_2 - Rb_{\text{in,op}}, \\ a''_1 &= Ta'_1 - RTb_{\text{in,op}} - R^2a'_2. \end{aligned} \quad (\text{S15})$$

The total effects of the two delay lines are:

$$\begin{aligned} a_1'' &= T^2 a_1 - T^3 R b_{\text{in}} - R T b_{\text{in,op}} - R^2 T a_2 + R^4 a_1, \\ a_2'' &= T^2 a_2 - T^2 R b_{\text{in}} - T R^2 a_1 - R b_{\text{in,op}}. \end{aligned} \quad (\text{S16})$$

After passing the two-delay lines with opposite scattering order, the collective mode $(a_1 - a_2)$ becomes,

$$\begin{aligned} a_1'' - a_2'' &= T(T + R^2)(a_1 - a_2) - R T^2(T - 1)b_{\text{in}} - R(T - 1)b_{\text{in,op}} + R^4 a_1 \\ &\approx (a_1 - a_2) + o(R^2). \end{aligned} \quad (\text{S17})$$

This collective mode is unchanged up to second order in T . Therefore, two delay lines with different directions can form a dark mode. The collective mode with opposite relative phase $(a_1 + a_2)$ experiences loss through these delay lines:

$$\begin{aligned} a_1'' + a_2'' &= T(T - R^2)(a_1 + a_2) - R T^2(T + 1)b_{\text{in}} - R(T + 1)b_{\text{in,op}} + R^4 a_1 \\ &\approx (1 - R^2)(a_1 + a_2) - R(b_{\text{in}} + b_{\text{in,op}}) + o(R^2). \end{aligned} \quad (\text{S18})$$

Note that Eq. (S18) is equivalent to the coupling between a loss channel $b_{\text{in}} + b_{\text{in,op}}$ and a collective mode $(a_1 + a_2)$. The collective loss Eq. (S18) can also be expressed by the Lindblad terms:

$$\begin{aligned} \mathcal{L}_{1,2}(\rho) &= \frac{\Gamma_c}{2}(2L_{1,2}\rho L_{1,2}^\dagger - L_{1,2}^\dagger L_{1,2}\rho - \rho L_{1,2}^\dagger L_{1,2}), \\ L_{1,2} &= a_1 + a_2. \end{aligned} \quad (\text{S19})$$

Note that the preferred collective mode can be changed by including an electro-optic phase and amplitude modulator (EOM),

$$L_{1,2} = a_1 + a_2 \longrightarrow L'_{1,2} = a_1 - a_2. \quad (\text{S20})$$

B. Multi-mode collective loss for frustration elimination

To eliminate the frustration in CIMs, we need a frustration-eliminating loss channel of the following form:

$$L_{\text{ani}} = \sum_{n,m} e^{i\phi_{m,n}} (a_n + \text{sign}(J_{m,n})a_m) + 2a_{\text{ani}}. \quad (\text{S21})$$

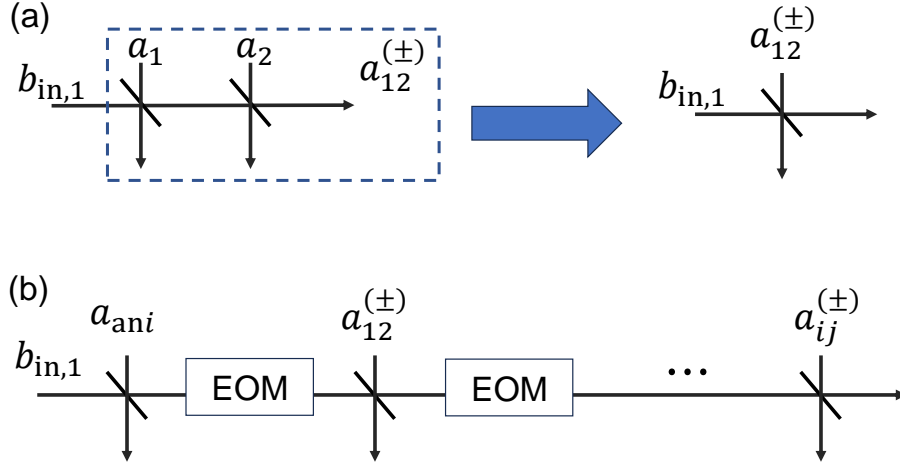


FIG. 3: Illustration of the multi-port delay line. (a) Expression of two modes coupled to a delay line as a collective mode. (b) Illustrations of phase terms in the frustration-eliminating channel generated by the phase and amplitude modulators (EOM). A multi-port delay line can be naively interpreted as connecting several two-port delay lines with EOMs.

Note that here we take the frustration-eliminating channel of an idler ancillary mode as an example, while the channel for the signal ancillary modes only differs in the phases. Such loss can be realized by multi-port delay lines, as illustrated in Fig. 3.

To simplify the expressions, we express the two signal modes coupled to the delay line in Fig. 1 as a collective mode, as shown in Fig. 3(a). Note that

$$a_{12}^{(\pm)} = a_1 \pm a_2. \quad (\text{S22})$$

We can couple multiple collective modes, which correspond to different coupling terms in Eq. (S8), to a common open-port delay, as illustrated in Fig. 3(b). By introducing necessary phase terms $\phi_{m,n}$ with EOMs, the collective mode coupled to the delay line is exactly the Lindblad operator in Eq. (S21). The additional coupling terms can be cancelled by a delay line in opposite direction as illustrated in Fig. 4.

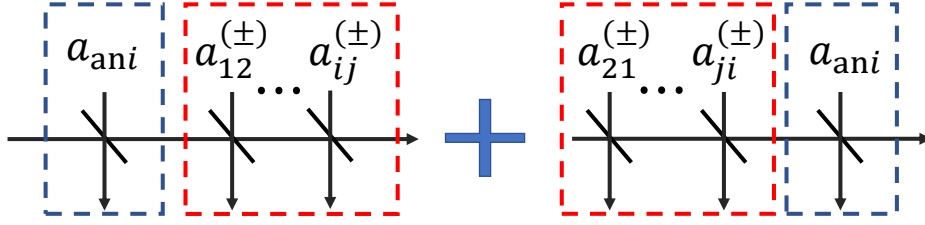


FIG. 4: Illustration of the frustration-eliminating loss channel formed by a pair of multi-port delay lines. As in the two-port delay cases, the unwanted coupling terms can be eliminated with a delay line in opposite direction.

IV. FRUSTRATION ELIMINATION IN MEASUREMENT-FEEDBACK COUPLING

Following the idea in Eq. (S11), the frustration-elimination coupling can also be realized with measurement feedback.

$$H_{\text{FEMF}} = i\Omega\langle(L_{\text{ani}} + L_{\text{ani}}^\dagger)\rangle(L_{\text{ani}} - L_{\text{ani}}^\dagger). \quad (\text{S23})$$

Consider now the semi-classical amplitude equation of the n th DOPO mode under the influence of this Hamiltonian,

$$\begin{aligned} \frac{\partial}{\partial t}\langle a_n \rangle &= i\langle[H_{\text{FEMF}}, a_n]\rangle, \\ &= -\Omega\langle(L_{\text{ani}} + L_{\text{ani}}^\dagger)\rangle\langle[(L_{\text{ani}} - L_{\text{ani}}^\dagger), a_n]\rangle \end{aligned} \quad (\text{S24})$$

Note that the contribution of the frustration-elimination loss in Eq. (S21) to the amplitude equation has a similar form in the semi-classical limit,

$$\begin{aligned} \frac{\partial}{\partial t}\langle a_n \rangle &= \frac{\Gamma_c}{2}\langle a_n(2L_{\text{ani}}\rho L_{\text{ani}}^\dagger - L_{\text{ani}}^\dagger L_{\text{ani}}\rho - \rho L_{\text{ani}}^\dagger L_{\text{ani}})\rangle, \\ &= \frac{\Gamma_c}{2}\langle[a_n, L_{\text{ani}}]\rho L_{\text{ani}}^\dagger\rangle + \frac{\Gamma_c}{2}\langle[L_{\text{ani}}^\dagger, a_n]L_{\text{ani}}\rho\rangle, \\ &\approx -\frac{\Gamma_c}{2}\langle L_{\text{ani}} + L_{\text{ani}}^\dagger\rangle\langle[(L_{\text{ani}} - L_{\text{ani}}^\dagger), a_n]\rangle. \end{aligned} \quad (\text{S25})$$

V. SCALING OF FRUSTRATION ELIMINATION DISSIPATIVE COUPLING

A. Including many coupling terms in one channel

Note that the number of distinguishable phases in Eq. (S21) is, due to the finite uncertainty of the coherent states, limited by the condition:

$$\langle \exp(i\phi_{m,n})|\alpha\rangle\langle \exp(i\phi_{m',n'})|\alpha\rangle \approx 0.$$

Therefore, to map large Ising models into the frustration-elimination scheme, it is necessary to attribute subgroups of couplings to several different loss channels. We assume that the coupling terms are divided into N_c different channels. The Lindblad operator of the k th channel can be designed as follows:

$$L_{\text{ani}}^{(k)} = \sum_{\{n,m\} \in C_k} e^{i\phi_{m,n}} [a_n + \text{sign}(J_{m,n})a_m] + (a_{\text{aniref}} + a_{\text{ani}}^{(k)}), \quad (\text{S26})$$

where C_k is a set describing the coupling terms in the k th loss channel. When the modes corresponding to the reference ancillary mode a_{aniref} and the k th ancillary mode $a_{\text{ani}}^{(k)}$ have the same phase, one of the coupling terms in this channel can be flipped, while no coupling term is flipped for opposite phases. Therefore, if not more than one ancillary mode $a_{\text{ani}}^{(k)}$ has the same phase as the ancillary reference mode a_{aniref} , these loss channels have the same effect as a single overall frustration-elimination loss channel containing all the coupling terms.

To realize the desired configuration of the ancillary modes and the ancillary reference mode, we can apply the following collective loss channel:

$$L_{\text{anicontrol}} = (N_c - 2)a_{\text{aniref}} - \sum_{k=1}^{N_c} a_{\text{ani}}^{(k)}. \quad (\text{S27})$$

When the amplitudes of all the modes have the same absolute values, only a single ancillary mode can have an opposite phase relative to the reference ancillary mode in the dark collective modes $L_{\text{anicontrol}}|\psi\rangle = 0$.

B. Including many ancillary modes in one channel

In order to flip $N_f > 1$ coupling terms, N_f ancillary modes are required. In this case, we need to exclude the occurrence of unwanted collective dark modes. It is instructive to first

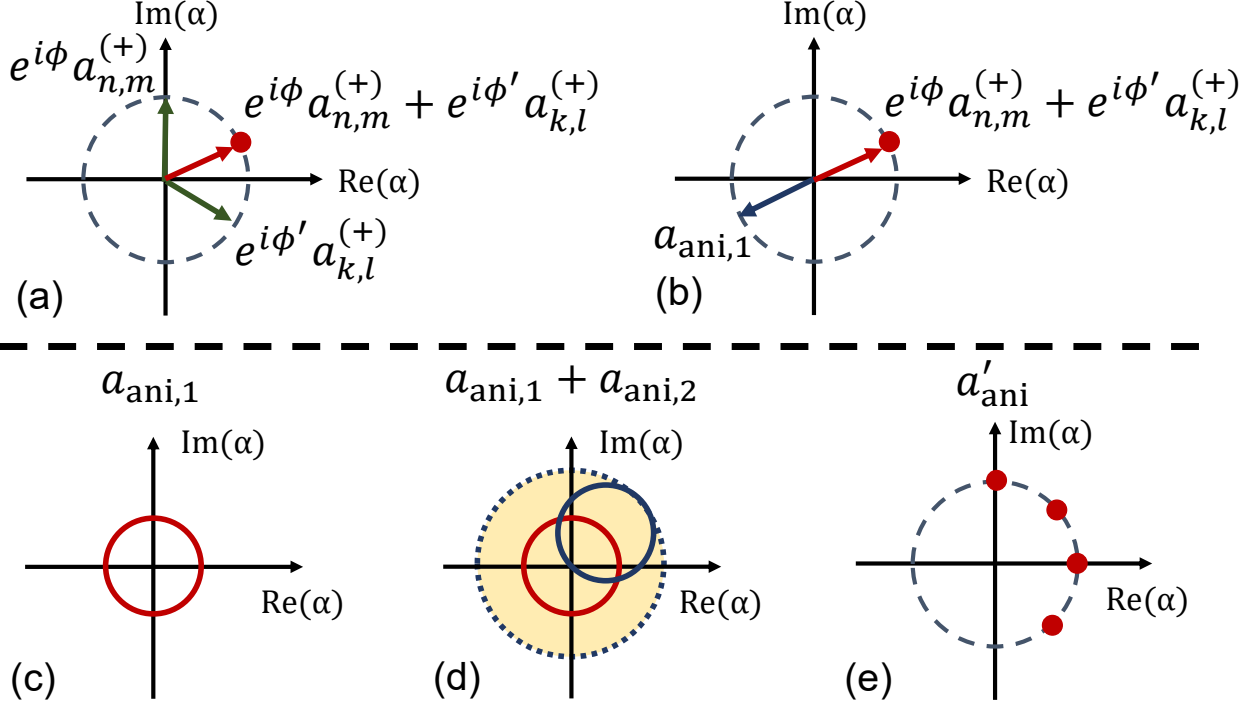


FIG. 5: Illustration of unwanted collective dark modes in frustration elimination set-ups and the corresponding solution. (a) Improper choices of phase terms can result in a collective mode which is equivalent to an addition coupling term in Eq. (S21). (b) Flipping the collective mode in Fig. 5(a) can change the sign of two coupling terms in Eq. (S21). (c) The phase space covered by a NDOPO mode. (d) The phase space covered by the sum of two NDOPO modes. (e) Discrete distribution proposed to reduce the area covered by NDOPO modes. Further constraints on NDOPO modes are necessary to avoid unwanted solutions when we want to flip more than one coupling terms.

discuss the occurrence of unwanted collective dark modes for the case of a single ancillary mode. Figures 5 (a) and (b) illustrate an example of such an unwanted collective dark mode. Assume that there are two coupling terms $a_{n,m}^{(+)}$, $a_{k,l}^{(+)}$, and one ancillary mode $a_{\text{ani},1}$. In this configuration, the ancillary mode should flip one of the coupling terms. However, if the phases corresponding to the coupling terms are not properly chosen, these two coupling terms can form a collective mode

$$e^{i\phi} a_{n,m}^{(+)} + e^{i\phi'} a_{k,l}^{(+)},$$

on the circle covered by the ancillary mode $a_{\text{ani},1}$, as illustrated in Fig. 5(a). In such a case, the ancillary mode $a_{\text{ani},1}$ can flip these two coupling terms simultaneously, as shown in Fig. 5(b), which results in a wrong output. However, when there is only one ancillary mode,

such problem can be avoided by choosing a suitable arrangement of the phases $\phi_{m,n}$.

If more than one ancillary mode are required to flip many coupling terms, there can be additional unwanted collective dark modes. One NDOPO mode can cover a circle in phase space, as shown in Fig. 5(c). To avoid unwanted solutions, all the sums of the coupling terms, e.g., $e^{i\phi} a_{n,m}^{(+)} + e^{i\phi'} a_{k,l}^{(+)}$, should not be located on this circle. However, the sum of two NDOPO ancillary modes can cover a disk in phase space, as illustrated in Fig. 5(d), which will inevitably cover some sums of the coupling terms.

One possible solution to this problem is to restrict the phase of the ancillary modes to discrete values, as shown in Fig. 5(e), where each point corresponds to a coupling term in Eq. (S21). Since there is only a finite number of phase space points that emerge as sums of two such discrete ancillary modes, it would be possible to avoid unwanted solutions.

A possible method to restrict the phases of the the ancillary modes to discrete values is by applying an additional loss channel with the form as in Eq. (S21):

$$L_{\text{control}} = \sum_{n,m} e^{i\phi_{m,n}} (a_{\text{control},n} + a_{\text{control},m}) + 2a_{\text{ani}}. \quad (\text{S28})$$

The control DOPO modes describe a frustrated Ising model, which can be turned into a model without frustration by flipping one coupling term. As a result, the ancillary mode can only pick up the phases in this channel.

-
- [1] M. Wolinsky and H. J. Carmichael, Phys. Rev. Lett. **60**, 1836 (1988), URL <https://link.aps.org/doi/10.1103/PhysRevLett.60.1836>.
 - [2] P. D. Drummond and K. Dechoum, Phys. Rev. Lett. **95**, 083601 (2005), URL <https://link.aps.org/doi/10.1103/PhysRevLett.95.083601>.
 - [3] A. Marandi, Z. Wang, K. Takata, R. L. Byer, and Y. Yamamoto, Nature Photonics **8**, 937 (2014), URL <https://doi.org/10.1038/nphoton.2014.249>.
 - [4] P. L. McMahon, A. Marandi, Y. Haribara, R. Hamerly, C. Langrock, S. Tamate, T. Inagaki, H. Takesue, S. Utsunomiya, K. Aihara, et al., Science **354**, 614 (2016).
 - [5] T. Leleu, Y. Yamamoto, P. L. McMahon, and K. Aihara, Phys. Rev. Lett. **122**, 040607 (2019), URL <https://link.aps.org/doi/10.1103/PhysRevLett.122.040607>.